DOI: https://doi.org/10.68732/51413bb6fa7d49f7

ISBN: 978-9989-2053-6-1

Resolution-induced uncertainty in DEM-predicted brittle damage thresholds in sandstone

Jinci Chen[1, 3], Elli-Maria Charalampidou[1], Ali Ozel[2], James Woodman[4] & Audrey Ougier-Simonin[3]

[1] *Institute of GeoEnergy Engineering, School of Energy, Geoscience, Infrastructure and Society, Heriot-Watt University,Edinburgh, UK*
[2] *School of Engineering and Physical Sciences, Heriot-Watt University, Edinburgh, UK*
[3] *British Geological Survey, Keyworth,Nottingham, UK*
[4] *Geo-Design Consulting Engineers Ltd, Ringwood, UK*

jc2138@hw.ac.uk
0009-0002-0920-9778

Abstract

Brittle damage thresholds predicted by discrete element method (DEM) modelling are informative for interpreting rock failure processes and supporting engineering design. Nonetheless, these predictions are constrained by the model particle resolution. This study investigates whether variations in model particle resolution affect the interpretation of damage thresholds in sandstone subjected to uniaxial compression. A recently developed Subspring Network Breakable Voronoi model was used to simulate uniaxial compression at four different particle resolutions. The results show a systematic dependence of the predicted response on model particle solution. With increasing resolution, the predicted uniaxial compressive strength, crack initiation, and crack damage thresholds generally increase, while Young's modulus decreases slightly and Poisson's ratio shows limited sensitivity. Finer resolutions also produce significantly higher crack counts and denser fracture patterns. Despite these variations, the dominant macroscopic failure mode remains tensile dominated; axial splitting is observed across all resolutions. These findings indicate that model particle resolution influences quantitative interpretations of brittle damage more strongly than qualitative identification of failure modes. Consequently, model particlere solution should not be treated merely as a numerical setting but rather as a source of modelling uncertainty in DEM based rock engineering analyses. An intermediate model particle resolution is considered to provide a practical compromise between computational efficiency and representative failure behaviour.

Keywords

Brittle fracture, Model particle resolution, Damage threshold, Rock failure, Modelling uncertainty.

1 Introduction

Rock engineering design and risk assessment are commonly informed by discrete element method (DEM) predictive modelling. Thus, accurate calculations and predictions of brittle damage onset, unstable crack growth, and peak strength appear to be crucial for informed design decisions.

DEM based Bonded-Particle Models (BPMs) have demonstrated sufficient flexibility and capability to accurately reproduce the brittle fracture process in both compact and porous rocks (Potyondy and Cundall 2004; Potyondy 2012; Potyondy et al. 2025). However, the selection of model particle scale can introduce uncertainty, thereby impacting the engineering assessment of rock damage thresholds and strength.

Conclusions drawn from modelling single particle resolution may lead to either overestimation or underestimation of damage initiation and instability thresholds. This uncertainty may affect risk management in rock engineering. Prior research has identified this issue as a particle size sensitivity problem (Peng et al. 2021; Zhang et al. 2022; Li et al. 2024; Sun et al. 2024; Potyondy and Fu 2024), although limited investigations have addressed the influence of discretisation-dependent responses on engineering interpretation.

This paper uses the recently established Subspring Network Breakable Voronoi (SNBV) model (Rasmussen 2021; Potyondy et al. 2025) to study the uniaxial compression of cylindrical specimens of sandstone. Model particle resolution can be expressed through specimen resolution (φ), defined in the current 3D SNBV model as the number of Voronoi particles spanning the specimen diameter. Four different specimen resolutions were examined. By quantifying the influence of φ on key damage and strength thresholds in sandstone, we aim to understand how these results affect engineering interpretation.

2 Computational model configuration

The SNBV model represents rock microstructure using a Voronoi tessellation, where Voronoi particles are bonded by linear elastic subsprings distributed across each particle interface. This model has two main features: first, it explicitly accounts for rock heterogeneity through the application of the Weibull probability distribution; second, it incorporates a grain breakage scheme that supports both inter- and intra-granular crack mechanisms. In this study, the model configuration was defined in terms of specimen geometry, porosity, particle size, and particle-size distribution. To ensure consistency with the laboratory data for Thornhill Rock reported by Woodman (2020) and Woodman et al. (2021), the specimen dimensions were set to 120 mm × 54 mm (height × diameter). A Weibull shape factor of m = 7.6 was adopted, based on values fitted to the indirect tensile strength distribution (Woodman et al. 2021). Additional heterogeneity sensitivity simulations (not shown here) indicate that, for the level of heterogeneity considered (m=7.6), the macroscopic response is only weakly affected. The influence of heterogeneity was therefore not considered further in the present study. Further details of the model formulation and implementation are provided by (Itasca Consulting Group, Inc. 2025).

Table 1. Model particle size configuration in the SNBV model.

Model	Initial seed diameter (mm)	Model particle size (mm)	Specimen resolution (φ)
Analogue 1	3.6	5.4	10
Analogue 2	2.4	3.4	15
Analogue 3	1.8	2.7	20
Analogue 4	1.2	1.8	30

In the present SNBV model, porosity was assumed to be zero due to the dense interlocking Voronoi microstructure. In contrast, Thornhill Rock has a reported grain size range of 63-250 μm and a porosity of approximately 15.5%. Poisson's ratio was implemented through fictitious stress corrections (Rasmussen et al. 2018). The cylindrical model was generated in three steps: (1) generation of non-overlapping spheres as initial seeds with a uniform distribution; (2) application of a Laguerre tessellation using these spheres as seeds, where the seed sizes influence the Voronoi cell size; and (3) trimming of the tessellated particles/blocks to produce a cylindrical specimen. Table 1 summarises the four model particle sizes, defined here as the mean diameter of the Voronoi particles

after trimming. Specimen resolution was calculated as the number of Voronoi particles spanning the cylinder diameter. We considered four initial seed diameters corresponding to four specimen resolution cases (see Table 1).

Compression simulations were performed by moving two rigid walls at the top and bottom towards each other. The frictional coefficient between model specimen and wall is set at 0.02 to reduce end effects. Damping ratio is 0.7, this is for energy dissipation and reduce dynamic effect. The loading rate was chosen to be slow enough to produce a quasi-static response, representative of the strain rate commonly adopted in laboratory rock testing ($10^{-5}$to 10^{-3} s^{-1}; (Paterson and Wong 2005)). It should be noted that, because mechanical timestep scaling was used, model time was not assumed to correspond directly to physical time. Axial strain was calculated from cumulative wall displacements, while axial stress was obtained by dividing the total reaction force acting on the loading walls by its contact area. Lateral strain was determined from radial deformation measurements obtained using circular ring blocks around the specimen diameter. These ring blocks were formed by the outermost Voronoi particles adjacent to the cylindrical specimen boundary, and their average was taken as the overall lateral strain. Simulations were performed using the three-dimensional Particle Flow Code, version 9.3 (Itasca Consulting Group, Inc. 2025).

3 Results

In this section, we discuss how varying specimen resolution (φ) affects macroscopic mechanical response. Each case was repeated three times with different random seed distributions while keeping other input parameters constant and only altering the particle size during model generation. All tests were conducted under consistent physical and boundary conditions throughout the study (e.g., model configuration and loading rate). It should be noted that variations in model particle size may affect the arrangement and interlocking of the grains, thereby affecting the packing fabric; however, these effects are not considered explicitly in the present study.

φ = 15 (blue curve in Fig.1) was adopted as the reference calibration case, as this intermediate resolution was considered representative by Potyondy et al. (2025). Its input parameters were calibrated against the specimens 235 and 207. All specimen resolutions reproduce the main macroscopic features of the experimental response, including crack closure (CC), crack initiation (CI), crack damage (CD) and post-peak stress drop. A clear resolution dependence is observed: as resolution increases, the predicted peak stress progressively increases. In addition, the finer resolution models reach their peak strength at a larger axial strain than their coarser counterparts. The coarsest model underestimates the peak strength, while the finest model tends to overestimate both the peak stress and the strain at peak. These results indicate that φ has a non-negligible impact on themacroscopic mechanical behaviour, which motivates the subsequent analysis of damage thresholds.

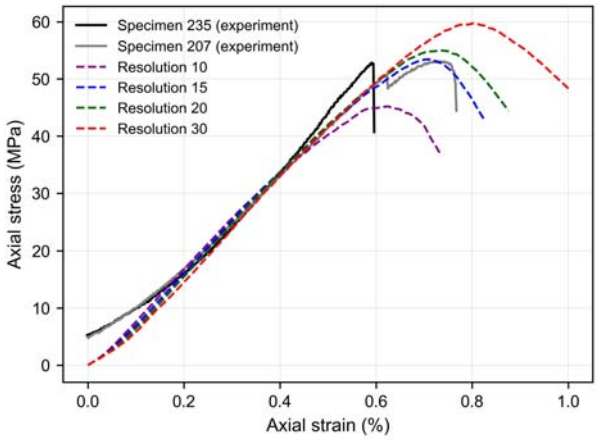


Fig.1 Comparison of axial stress-strain curves from laboratory UCS tests (specimens 235 and 207; Woodman et al. (2021)) and simulations at four specimen resolutions (see Table 1). The experimental curves include a small initial preload used to establish platen-specimen contact.

As the macroscopic stress-strain curves in Fig.1 show a clear dependence on specimen resolution, Fig. 2 quantifies this effect through derived damage thresholds. The CC, CIand CD thresholds were identified from the axial and volumetric strain responses (Nicksiar and Martin 2012). Young's modulus (E) and Poisson's ratio (ν) were determined over the linear interval between CC and CI. The

UCS, CI and CD values show an increasing trend with increasing specimen resolution, indicating that finer model particle size predict higher stress levels for the onset and progression of brittle damage. By contrast, *E* shows a slight decreasing trend, whereas *v* varies only within a narrow range and appears less sensitive to resolution changes. The scatter between repeat simulations remains relatively limited compared with the systematic change in the mean values, suggesting that the observed trend is primarily resolution driven rather than a consequence of random seeds generation alone.

This trend is observed under the specific condition that only the model particle size is varied, while maintaining consistent input parameters across all resolutions. In this study, φ=15 was used as the reference calibration case. Nonetheless, if a different specimen resolution was used as the calibration case, the resulting trend could differ because changes in packing fabric may require adjustments to the input parameters to reproduce the laboratory responses of specimens 235 and 207. In other words, although the model at a given resolution can be calibrated to match the experimental results, it should not be assumed that it will provide same quantitative predictive damage thresholds at other resolutions without any further recalibration. This issue is not confined to the laboratory scale, but also applies to engineering scale interpretation, where differences in discretisation, geometry and loading conditions may similarly affect the parameter set required to reproduce the target response.

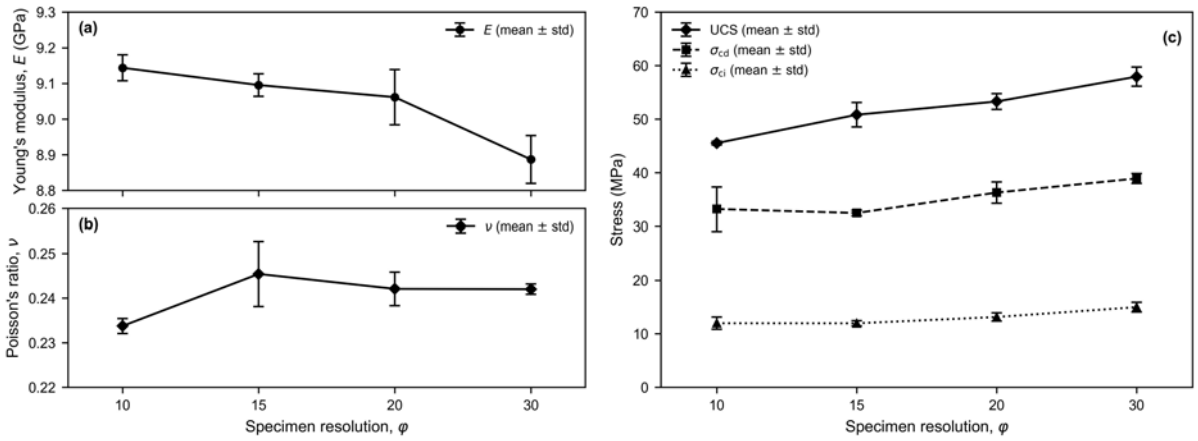


Fig. 2 The dependence of the key mechanical and damage indicators derived from simulations on specimen resolution (φ), including CC, CI, CD, *E*, *v*and UCS. Error bars show the scatter from three repeat runs.

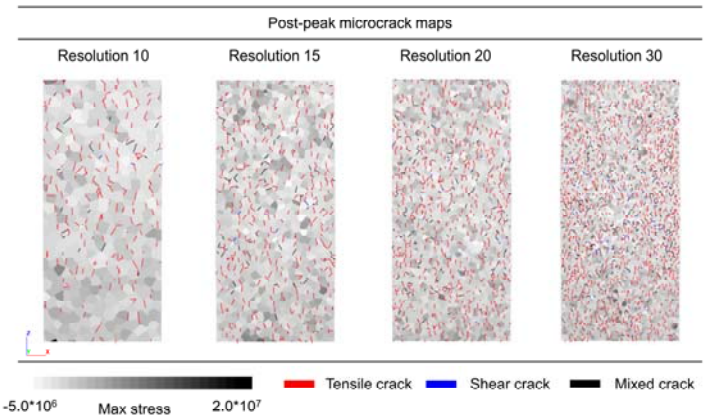


Fig. 3 Fracture traces of tensile, shear and mixed-mode microcracks on the central Z–X cross-section at the post-peak stage for four specimen resolutions.

To visualise damage distribution, Fig. 3 displays crack maps on the central Z–X cross-section of the cylindrical model at the post-peak stage. These maps represent the fracture traces observed on this section. The crack patterns are compared across different specimen resolutions, with Z denoting the specimen height axis and X the radial direction. Fig. 4 summarises the corresponding crack-type proportions and total crack counts. As specimen resolution increases, the total number of recorded crack events rises markedly, producing progressively denser fracture patterns in the finer discretisation. Despite this increase in crack density, the dominant failure pattern remains broadly consistent across the considered resolutions, with tensile cracking prevailing and the specimen exhibiting axial splitting. Fig. 4 further shows that across all resolutions, tensile cracks constitute the largest portion of the crack

population; however, their proportion declines modestly as the fractions of shear and mixed-mode cracks increase.

These results indicate that specimen resolution may alter the extent of crack accumulation but has limited effects on the overall failure mechanism. We speculate that an intermediate specimen resolution may still capture the representative failure mode, even though the predicted crack density and the associated threshold values remain resolution dependent. Based on these results, the trends in Fig. 2Fig. 3Fig. 4 show that specimen resolution influences the quantitative assessment of brittle damage more strongly than the qualitative identification of the failure mechanism. Increasing the resolution introduces more, smaller Voronoi particles and bonded contacts, expanding the number of potential crack paths and promoting more distributed bond breakage. This naturally leads to higher crack counts and shifts the predicted CI, CD and UCS to higher stress levels.

From a rock physics perspective, this distinction is crucial: while a single specimen resolution may still capture the representative failure mode, it may not provide resolution-independent estimates of damage thresholds used to interpret the onset and progression of instability. Since the simulations do not explicitly reproduce the true grain size of the tested sandstone, we adopted a larger but computationally affordable range of model particle size and examined their effect on four different specimen resolutions. The resulting particle size effects, defined by specimen resolution, align with trends reported in experimental studies where finer-grained rock materials typically exhibit higher strengths. In this sense, the behaviour observed in higher resolution simulations resembles that of experimentally tested samples with smaller grain sizes and, in some cases, lower porosity.

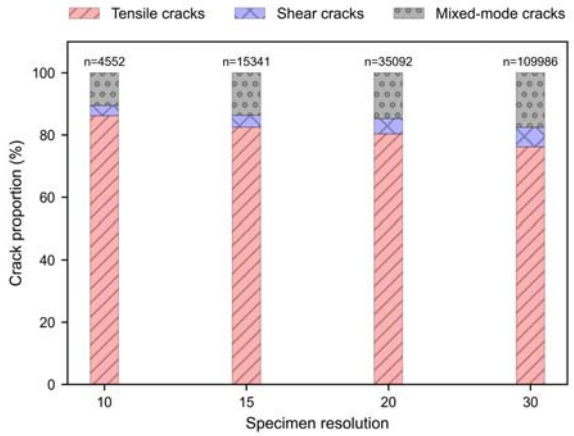


Fig. 4 Proportions of tensile, shear and mixed-mode cracks for different specimen resolutions at the post-peak stage; n above each bar denotes the total crack count.

4 Conclusions

This study investigates the influence of specimen resolution on the mechanical response and damage thresholds of sandstone subjected to uniaxial compression using the SNBV model. The main conclusions are as follows.

(1) Specimen resolution has a systematic effect on the predicted UCS values and associated damage thresholds.
(2) The predicted UCS, CI and CD thresholds generally increase with increasing specimen resolution, whereas Young's modulus shows a slight decrease and Poisson's ratio is comparatively less sensitive.
(3) Although crack density increases markedly at higher specimen resolutions, the dominant failure mode remains tensile dominated as axial splitting is observed across the resolutions considered, indicating that the model can capture well the occurring macroprocesses.

These results suggest that specimen resolution should not be treated merely as a numerical setting but rather as a source of modelling uncertainty that affects the inferred onset and propagation of brittle damage. Using an intermediate specimen resolution still reveals critical damage features while maintaining a practical balance between computational efficiency and representative failure response.

References

Itasca Consulting Group, Inc. (2025) Subspring network model. PFC Documentation. Available at: https://docs.itascacg.com/itasca940/common/contactmodel/rbsn/doc/manual/cmspringnetwork.html?node5092. Accessed 25 May 2026.

Li W, Yu L, Zhang T, Su H, Mi X, Fan D, Jin B (2024) Quantitative analysis of grain size effect on tensile mechanical behavior of granite based on multi-level force chain networks. *Computational Particle Mechanics*, 11(5): 2245–2266.DOI:10.1007/s40571-024-00790-3

Nicksiar M, Martin C (2012)Evaluation of methods for determining crack initiation in compression tests on low-porosity rocks.*Rock Mechanics and Rock Engineering*, 45(4): 607–617.DOI: 10.1007/s00603-012-0221-6

Paterson MS, Wong TF (2005)*Experimental Rock Deformation – The Brittle Field*.2nd edn.Springer,Berlin Heidelberg.

Peng J, Wong LNY, Teh CI (2021) Influence of grain size on strength of polymineralic crystalline rock:Newinsights from DEM grain-based modeling. *Journal of Rock Mechanics and Geotechnical Engineering*, 13(4): 755–766.DOI:10.1016/j.jrmge.2021.01.011

Potyondy DO, Cundall PA (2004) A bonded-particle model for rock. *International Journal of Rock Mechanicsand Mining Sciences,* 41(8): 1329–1364. DOI:10.1016/j.ijrmms.2004.09.011

Potyondy DO (2012)A flat-jointed bonded-particle material for hard rock.*46th US Rock Mechanics/Geomechanics Symposium*,Chicago, Illinois, USA,24–27 June 2012,Paper No. ARMA-2012-501.

Potyondy DO, Fu W (2024)A 3D subspring network breakable Voronoi model for rock: laboratory-scale behavior.*58th US Rock Mechanics/Geomechanics Symposium*,Golden, Colorado, USA,23–26 June 2024,Paper No. D031S029R005.

Potyondy DO, Fu W, Purvance M, Mas Ivars D (2025) A 3D subspring network breakable Voronoi model for rock. *Rock Mechanics and Rock Engineering*. DOI: 10.1007/s00603-025-04655-w

Rasmussen LL (2021) Hybrid lattice/discrete element method for bonded block modeling of rocks. *Computers and Geotechnics*, 130: 103907. DOI:10.1016/j.compgeo.2020.103907

Rasmussen LL, de Farias MM, de Assis AP (2018) Extended Rigid Body Spring Network method for the simulation of brittle rocks. *Computers and Geotechnics*, 99: 31–41.DOI:10.1016/j.compgeo.2018.02.021

Sun Y, Kwok CY, Duan K (2024) Size effects on crystalline rock masses: Insights from grain-based DEM modeling. *Computers and Geotechnics*, 171: 106376. DOI:10.1016/j.compgeo.2024.106376

Woodman J (2020) *Thermo-mechanical loading of intact rock and discontinuities*. PhD thesis, University of Leeds. Available at: https://etheses.whiterose.ac.uk/id/eprint/26306/. Accessed 25 May 2026.

Woodman J, Ougier-Simonin A, Stavrou A, Vazaios I, Murphy W, Thomas ME, Reeves HJ (2021) Laboratory experiments and grain based discrete element numerical simulations investigating the thermo-mechanical behaviour of sandstone. *Geotechnical and Geological Engineering*, 39(7): 4795–4815.DOI:10.1007/s10706-021-01794-z

Zhang T, Yu L, Peng Y, Ju M, Yin Q, Wei J, Jia S (2022) Influence of grain size and basic element size on rock mechanical characteristics: insights from grain-based numerical analysis. *Bulletin of Engineering Geology and the Environment*, 81(9): 347.DOI:10.1007/s10064-022-02856-z